Microwave Power and Phase Measurements on a Recirculating Planar Magnetron

Matthew A. Franzi, *Student Member, IEEE*, Geoffrey B. Greening, *Student Member, IEEE,* Nicholas M. Jordan, *Member, IEEE*, Ronald M. Gilgenbach, *Life Fellow, IEEE,* David H. Simon, *Student Member, IEEE*, Y. Y. Lau, *Fellow, IEEE*, Brad W. Hoff, *Member, IEEE*, and John Luginsland, *Member, IEEE*

***Abstract*— Calibrated microwave power and phase measurements are presented for the first recirculating planar magnetron prototype consisting of two coupled six-cavity 1-GHz planar cavity arrays. The results are presented for a solid cathode and two mode-control cathodes (MCCs) with aluminum or velvet electron emitters. The measurements were conducted using a prototype coaxial microwave power extraction scheme. The experimental operating parameters included: pulsed cathode voltages between −250 and −300 kV, voltage pulselengths of 200–600 μs, axial magnetic fields of 0.1–0.32 T, and entrance currents of 1–10 kA. The results showed improved oscillator frequency locking for the MCCs and increases in power and efficiency using the velvet electron emitter.**

***Index Terms*— Cavity magnetron, frequency locking, high-power microwaves (HPMs), recirculating planar magnetron (RPM), vacuum electronics.**

I. Introduction

HIGH-POWER microwaves (HPMs) have important applications to fusion plasma heating [1], advanced radar, and potentially countering improvised explosive devices [2]. The optimal combination of compactness and high microwave power is generally recognized as the magnetron and its variant, the crossed-field amplifier (CFA) [3]. Thus, magnetrons and CFAs are utilized extensively in military systems, including the U.S. Navy's Aegis combat system and the Patriot missile system [4]. However, conventional magnetrons have several limitations when attempting to scale the microwave power to hundreds of megawatt or gigawatt levels at long pulses (microseconds to milliseconds), due in part to the geometry of the device. The concentric configuration of the anode and cathode in a cylindrical magnetron inherently limits the available surface area of both electrodes. This geometric limitation may restrict both the available current from the cathode as well as the ability to dissipate heat generated in the anode.

Researchers at the University of Michigan (UM) have invented and developed a new variant of the magnetron, the recirculating planar magnetron (RPM), which addresses many of the shortcomings of conventional magnetrons for HPM generation [5], [6]. Fig. 1(a) shows a photograph of

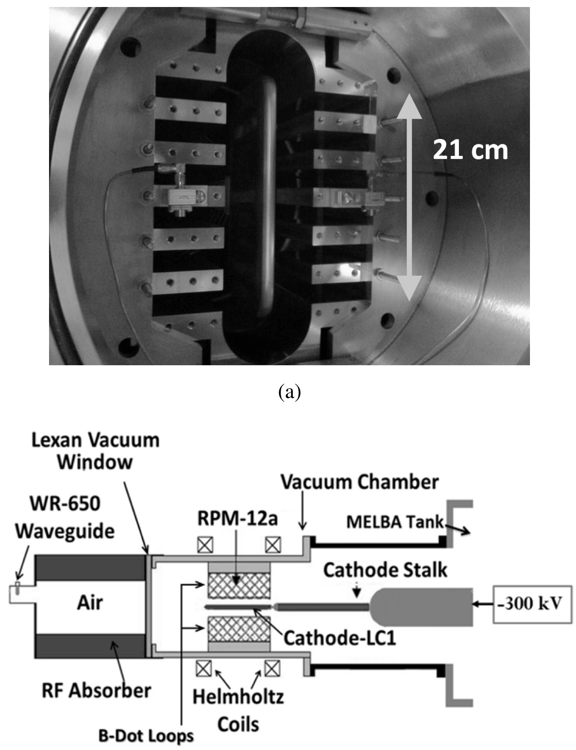

(a)

(b)

Fig. 1. Experimental configuration for the phase measurements. (a) Photograph of RPM-12A viewed from the front. The center plate is the LC-1 cathode. Anode periodic structures are to the left and right of the cathode. (b) Cross-sectional top view of the experimental setup for the RPM-12A phase measurements.

Manuscript received December 4, 2014; revised February 20, 2015; accepted March 15, 2015. Date of publication April 13, 2015; date of current version May 6, 2015. This work was supported in part by the Air Force Office of Scientific Research under Grant FA9550-10-1-0104, in part by the Air Force Research Laboratory, and in part by the L-3 Communications Electron Devices.

M. A. Franzi was with the Plasma, Pulsed Power, and Microwave Laboratory, University of Michigan, Ann Arbor, MI 48109 USA. He is now with SLAC National Accelerator Laboratory, Electrodynamics, Menlo Park, CA 94025 USA (e-mail: mfronz@umich.edu).

G. B. Greening, N. M. Jordan, R. M. Gilgenbach, D. H. Simon, and Y. Y. Lau are with the Plasma, Pulsed Power, and Microwave Laboratory, University of Michigan, Ann Arbor, MI 48109 USA (e-mail: geofgree@umich.edu; jordann@umich.edu; rongilg@umich.edu; dhsimon@umich.edu; yylau@umich.edu).

B. W. Hoff is with the Air Force Research Laboratory, Kirtland Air Force Base, Air Force Research Laboratory, Kirtland Air Force Base, Albuquerque, NM 87117 USA (e-mail: brad.hoff@kirtland.af.mil).

J. Luginsland is with the Air Force Office of Scientific Research, Arlington, VA 22203 USA (e-mail: john.luginsland@afosr.af.mil).

Digital Object Identifier 10.1109/TPS.2015.2417774

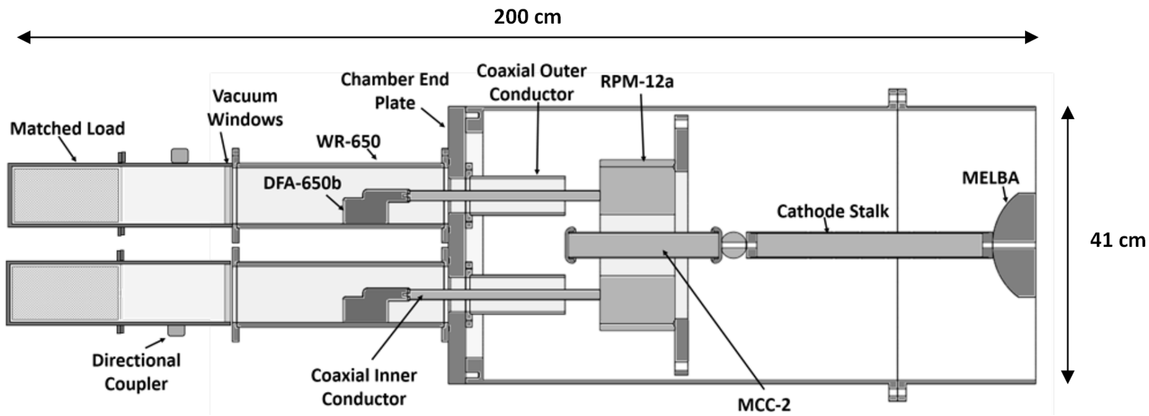

Fig. 2. Cross-sectional top view of the experimental setup for microwave power measurements with the prototype coaxial extraction system.

the UM RPM-12A, the first RPM prototype [7]. RPM-12A couples two planar 1-GHz magnetron oscillator sections with cylindrical bends permitting recirculation of RF and the electron beam.

The advantages of the RPM include:

1) larger cathode area yields much higher available electron current at a given current density;
2) larger anode area for improved heat dissipation;
3) decoupling of the design of the anode–cathode (AK) gap from the vane geometry;
4) scalability to higher powers by increasing the number of cavities (shown in simulations [8]);
5) decreased volume of magnetic field (scales as N) compared with that in conventional cylindrical magnetrons (scales as N^2), where N is the number of cavities.

Computer simulations and experiments at the UM have demonstrated that this unoptimized RPM device can operate as a relativistic magnetron with similar efficiencies as conventional cylindrical relativistic magnetrons [9]–[13].

In this paper, we present the first calibrated microwave power measurements and phase measurements for RPM-12A.

II. Experimental Configuration

The Michigan electron long beam accelerator with a ceramic insulator stack (MELBA-C) was used to operate RPM-12A at voltages between −250 and −300 kV for pulselengths of 200–600 μs. Pulsed electromagnets were placed approximately 21.6-cm apart in a pseudo-Helmholtz configuration and centered over the anode region to create a nearly uniform axial magnetic field, which was varied on a per-shot basis from 0.1 to 0.32 T. The magnetron was housed within a cylindrical, 63.5-cm long, 39.4-cm diameter, #304 stainless steel vacuum chamber and was operated at vacuums between 10^{-6} and 10^{-5} torr. The MELBA-C voltage pulse was sampled by a $CuSO_4$ resistive divider and the current entering RPM-12A was measured by a Rogowski coil embedded in the MELBA-C output port.

The phase measurements were obtained using signals generated by 2-mm^2 $\dot{B}$ loops installed on both oscillators approximately 4 mm axially from the central open-ended cavity of each of the RPM-12A anode slow-wave structures (SWSs), as shown in Fig. 1(b) [14]. The signals from each $\dot{B}$ loop were transmitted to the Faraday cage housing the data recording oscilloscopes by two identical RG-213U n-type cables. A 4-GHz, 20-GS/s Tektronix 7404 (Tek7404) oscilloscope was used to directly record the $\dot{B}$ signals.

Fig. 2 shows the experimental configuration for RPM-12A with the first iteration of the coaxial extraction system. Microwave output power was extracted via two symmetric coaxial waveguides (2.5-cm Outer Diameter (OD) and 0.75-cm Inner Diameter) whose inner conductors were mounted directly to the central vane of each oscillator of the RPM. Axially downstream from the magnetron, the coaxial transmission line was transitioned to WR 650 waveguide where the RF power was sampled by a directional coupler (−58 dB), and dissipated in an Ecosorb load. To observe and diagnose the operation and internal coupling between each oscillator, the output from each SWS was not externally combined. The sampled microwave signals were transmitted to the Faraday cage using two RG-213U n-type cables and attenuated by 20–25 dB using in-line attenuators. The signal was split using a two-way power divider to be: 1) directly sampled by the Tek7404 oscilloscope and 2) rectified by calibrated Agilent 8472B low-barrier Schottky diode microwave detectors, which were connected to a 500-MHz Tektronix 3054 oscilloscope for power measurement. Direct sampling via the Tek7404 captured the relative phase of the signals, as well as the time-dependent frequency information. While an endloss current measurement was not feasible for this extraction setup, endloss measurements were performed using a modification of the setup shown in Fig. 1(b) in which the Lexan output window was replaced with an electron beam collector. These measurements were used to estimate the endloss current for shots conducted using the configuration shown in Fig. 2.

Several cathode variations were used in this paper. The various cathodes are shown in Fig. 3. The first embodiment (Low Current (LC)-1) was a solid planar cathode 24-cm wide, 1.3-cm thick, and 15-cm deep. This cathode was tested with a bare aluminum surface with 10×2 cm strips of dielectric fiber in an emission-priming configuration [15].

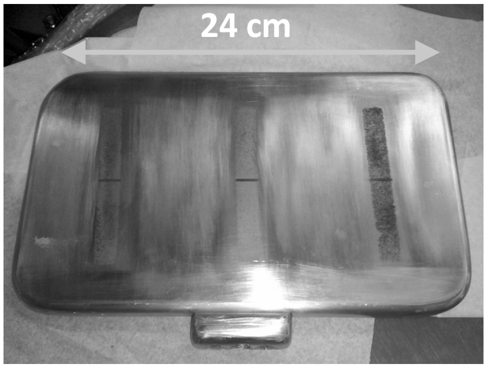

(a)

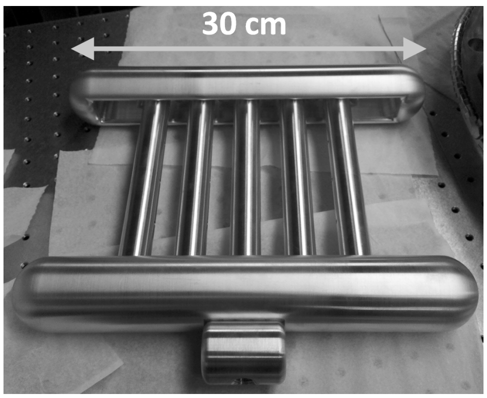

(b)

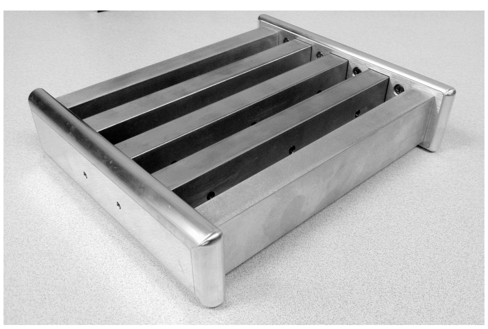

(c)

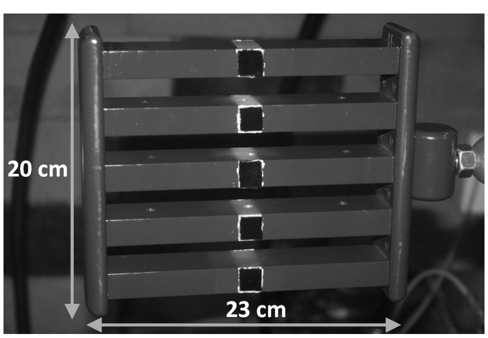

(d)

Fig. 3. Cathode designs and configurations. (a) LC-1. (b) MCC-1. (c) MCC-2. (d) MCC-2 with Glyptal paint and velvet emitters.

To improve mode separation, the mode-control cathode (MCC) was developed. While geometrically similar to the transparent cathode [16], the periodically slotted geometry of the MCC is unique in that it acted as both an emission-primed electron source as well as a resonant electromagnetic coupler, which facilitated the propagation of RF power from one oscillator to the other [17]. Two models of the MCC, designated as MCC-1 and MCC-2, were constructed for the operation in the unloaded RPM-12A experimental setup shown in Fig. 1. These two MCC models were evaluated against LC-1 on the basis of relative phase differences between symmetric cavities of each planar oscillator. A summary of the geometric parameters of these devices may be found in Table I.

TABLE I
CATHODE DESIGN PARAMETERS

Cathode	Effective Thickness [cm]	AK Gap [cm]
LC-1	1.3	3.9
MCC-1	2.2	3.4
MCC-2	3.8	2.6

TABLE II
FREQUENCY-LOCKING PERCENTAGE

Cathode	Locked $\pm 10^\circ$ [% of Shots]
LC-1	23
MCC-1	32
MCC-2	57

Both MCCs featured a periodic array of hollow aluminum emitters spaced 3.8-cm apart, matching the vane-cavity periodicity of the surrounding SWS to facilitate emission-priming of the electrode. The MCC-1 was designed using five (2.2-cm OD) cylindrical conductors, which provided an effective AK gap of 3.4 cm. Each rod was press-fit into two 25-cm long, 5.1-cm diameter end caps spaced 22-cm apart. The MCC-2, designed to reduce the effective AK gap of the RPM diode, was composed of five hollow, 1.9×3.8 cm rectangular structures, resulting in an AK gap of 2.6 cm. Including the end caps, it was 23 cm in length. To suppress undesirable emission, the end caps of both MCCs were coated with the Glyptal insulating paint. The final embodiment of the MCC-2 added $(1.9\ \text{cm})^2$ velvet squares to the center of the cathode using conductive silver epoxy adhesive.

III. EXPERIMENTAL RESULTS AND DISCUSSION

A. Phase Measurements

High-frequency noise on the $\dot{B}$ signals (>1.5 GHz) was numerically filtered and the time resolved phase of magnetron oscillations was extracted by application of a Hilbert transform to generate an analytic representation. Measurement inaccuracies were mitigated by restricting our analysis to only the relative phase difference between the two oscillators. Residual jitter and noise on the relative phase traces were removed using a moving average over a 5-ns window [18].

For the purposes of consistency, frequency locking was defined in our study as a state of operation wherein the relative phase difference between each oscillator was static for durations greater than 20 ns with a margin of error defined $\pm 10^\circ$. The data in Table II represent the percentage of shots having HPM pulselengths in excess of 100 ns that achieved this locked state during the operation.

The solid aluminum cathode (LC-1) facilitated some margin of coupling between oscillators via the cylindrical bends

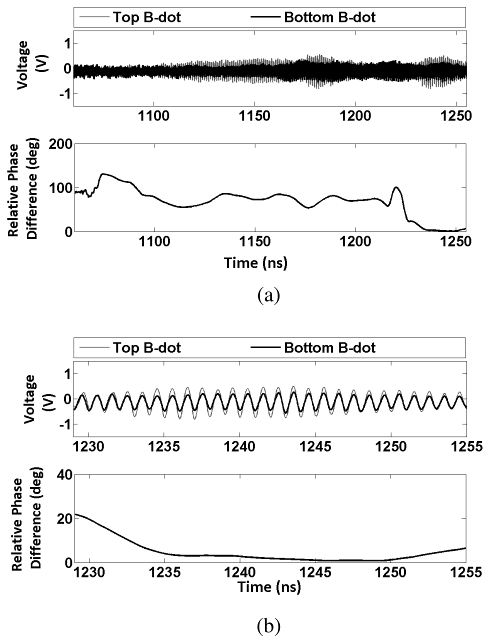

Fig. 4. Microwave oscillations sampled by the anode $\dot{B}$ loops plotted with the relative phase between each SWS. Here, the cathode variant was the MCC-1. (a) Onset of oscillations leading to a locked state. (b) Zoomed-in plot of the locked state above.

of RPM-12A and therefore exhibited instances of coherency between each oscillator. The LC-1 cathode, which featured no electromagnetic coupling through the electrode, was also highly susceptible to electron endloss. This limited both RF power and the ability of RPM-12A to frequency-lock [19]. The inclusion of end caps in the MCC-1 design, shown in Fig. 3(b), was observed to reduce parasitic current in the device from 1.5 kA to less than 0.2 kA, but resulted in a higher susceptibility to gap closure and subsequent pulse shortening. This behavior is consistent with [10] and [20] although there have been instances of end cap implementation that did not suffer an increase in gap closure susceptibility [14].

The MCC-1 was the first cathode prototype featuring electromagnetic coupling through the emitting structure and demonstrated a 9% increased propensity to achieve a state of frequency-locked operation. Frequency locking occurred, on average, 111 ns after the first oscillations were observed in RPM-12A and was typically toward the end of the microwave pulse. The time to achieve frequency locking was heavily influenced by mode competition in the device and, in some cases, extended to more than 180 ns when bimodal operation was observed. An example of this behavior is shown by the signal trace in Fig. 4.

The long frequency-locking times observed with the MCC-1 were attributed largely to the 3.4-cm AK-gap, which severely limited the cross-oscillator coupling provided by the cathode [17]. The analytic dispersion relation for RPM-12A with MCC-1 revealed a tightly spaced competitive mode structure where as little as 3-MHz separation exists between the even and odd π modes. Furthermore, the magnitude of the RF electric field on the cathode surface falls off with increased AK separation, thus limiting the RF power coupled to the opposing oscillator. Previous simulation work, using the 3-D particle-in-cell code MAGIC, showed that for AK gaps in excess of 3.0 cm, up to 150 ns of uninterrupted oscillation may be required to yield a fully locked state of operation. The improved performance of MCC-1, in comparison with that of LC-1, was indicative of both this minor improvement to the coupling between oscillators as well as a reduction in endloss current.

Improvements to the MCC-1 design were incorporated into the second prototype, MCC-2, which was described in the previous section. MCC-2 included a thicker body (approximately 3.8 cm) to reduce the AK gap from 3.4 cm (for the MCC-1) to 2.6 cm (for the MCC-2). MCC-2 also featured a more conservative end cap design intended to limit both parasitic current and plasma-induced gap closure, though the average microwave pulse length did not statistically improve.

RPM-12A with MCC-2, which achieved frequency locking on 57% of viable HPM pulses, demonstrated a significant improvement over MCC-1 (32%). Due to the improved performance of the MCC-2 over its experimentally tested predecessors, this cathode was exclusively tested as part of the power extraction study performed on RPM-12A.

B. Power Measurements

A total of 93 shots were conducted using the setup shown in Fig. 2 with the objective of measuring the output power. These shots were divided among two variations of MCC-2. In the first set, the emitter surface was 101 cm^2 of bare aluminum, and in the second set, the emitter surface area was replaced with 36 cm^2 of velvet fabric and conductive epoxy adhesive described in the experimental configuration section.

The voltages varied from -250 to -300 kV, with a brief overshoot at the peak of the pulse occasionally reaching as high as -330 kV. The range of magnetic fields was approximately 0.23–0.27 T for the aluminum emitter and 0.2–0.34 T for the velvet emitter.

Typical total currents entering the magnetron were 2–4 kA at the onset of oscillations. Due to the absence of an endloss current collector in the coaxial power extractor assembly, the precise endloss current during these shots was unknown. Quoted efficiencies in this paper are therefore total efficiencies, not electronic efficiencies.

An additional series of shots was conducted with an endloss collector in place of the extractor assembly (as described in the experimental configuration section). These showed typical endloss currents of less than 200 A, suggesting the end cap design of the MCC-2 cathode was effective at electrostatically confining the electron flow to the interaction region. Because the presence of the extractor does not significantly modify the fields surrounding the interaction region, it is unlikely that the endloss current changed significantly between the shots conducted with and without the presence of the coaxial power extractor assembly. Furthermore, the relatively small measured endloss currents suggest the peak electronic efficiencies were not substantially higher than the quoted total efficiencies below.

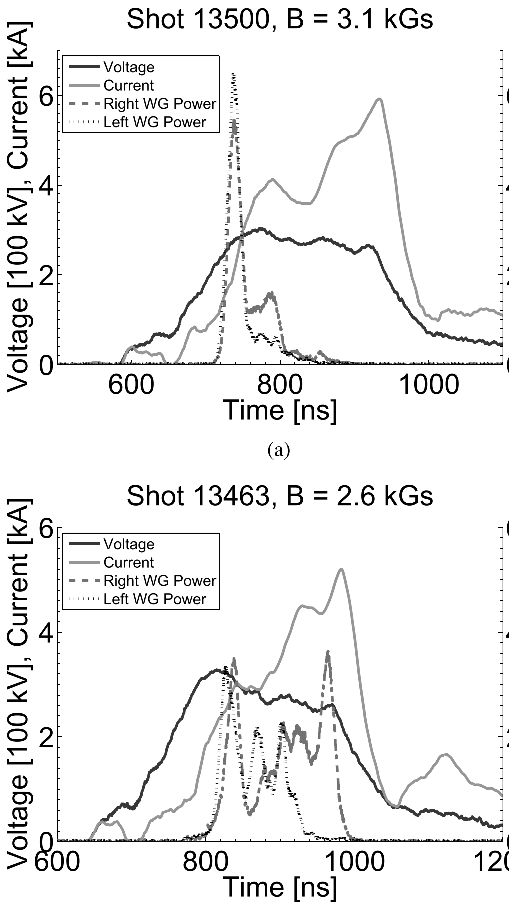

(a)

(b)

Fig. 5. Sample shots illustrating the two broad types of the RPM-12A operational behavior. (a) High-power, short-duration shot using the MCC-2 with a velvet emitter. (b) Low-power long-duration shot using the MCC-2 with a bare aluminum emitter.

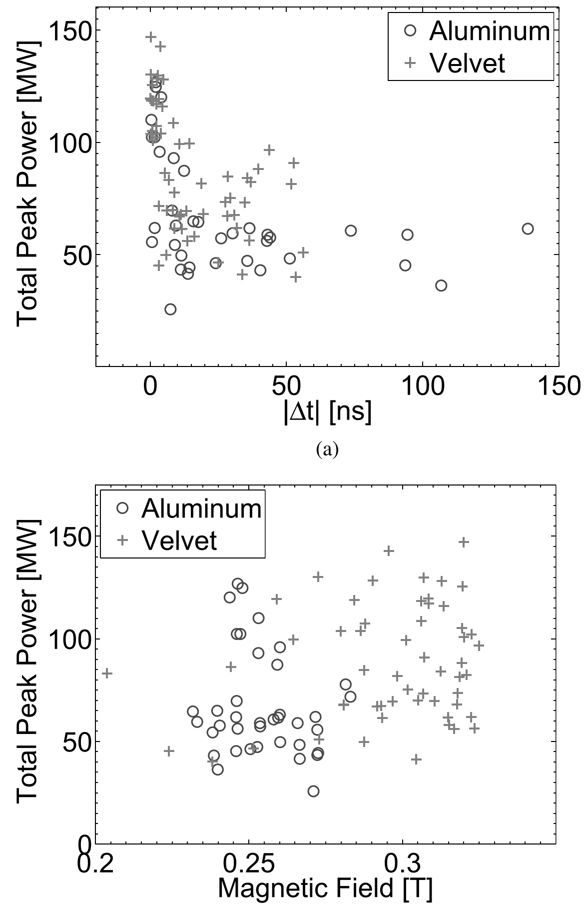

(a)

(b)

Fig. 6. Comparison of peak total powers using MCC-2 and bare aluminum or velvet emitters. (a) Peak total power versus $|\Delta t|$, where Δt is the difference in time between the peak output power for each waveguide. (b) Peak total power versus magnetic field for shots using MCC-2 with bare aluminum or velvet electron emitters.

Fig. 5 shows two sample shots with the total current, voltage, and detected RF power for each waveguide. A typical shot had a total voltage rise time between 100–150 ns.

The characteristic behavior of the current during the voltage ramp depended on the type of emitter. The bare aluminum typically drew less current during the voltage ramp than the velvet up to the onset of oscillations, at which point the current usually increased rapidly. The velvet usually experienced a smoother current ramp through the voltage rise time and the onset of oscillations. After oscillations ceased, current continued to increase steadily in a manner consistent with AK diode gap closure and space charge limited emission, which has been described at length in [14], [21], and [22].

Typical microwave diode detector signals were qualitatively similar for both the aluminum and velvet emitters. Shots for each emitter fell into two broad categories: high-power pulses (>100 MW) with short duration (<50 ns), and lower power pulses with longer duration. For this analysis, a high-power pulse refers to the total peak power, which is the peak of the sum of the two waveguide powers. Fig. 5(a) shows an example that falls into the former category, having a brief high-power burst for approximately 40 ns with lower powers for the remainder of the shot. Fig. 5(b) is an example that falls into the latter category, having a longer microwave pulse duration, but at lower powers. These shots also tend to exhibit greater mode hopping and mode competition.

The experimental results demonstrated clear differences in the RPM-12A performance between the bare aluminum and velvet emitters. The affected performance metrics include: consistency of simultaneous high-power oscillations for each of the SWSs, consistency of total power output, peak total efficiency, and oscillation start time.

The total peak power is strongly affected by the times at which each individual SWS reaches peak power output. This effect is shown in Fig. 6(a), which shows the peak total power versus $|\Delta t|$, where Δt is the difference in time between the peak output power for each individual RPM-12A section waveguide. High peak power shots (>100 MW) for both emitters only occurred when $|\Delta t|$ was very small, usually <5 ns. Table III shows the percentage of shots with $|\Delta t| < 5$ ns for each emitter.

Fig. 6(b) compares the peak total power versus magnetic field for the different emitters. The range of peak output powers was similar for both emitters. However, the aluminum emitter produced a low peak power (<100 MW) far more consistently than the velvet due to the decreased frequency of

TABLE III
PERFORMANCE METRICS FOR ALUMINUM AND VELVET EMITTERS

Emitter	Shots with $\|\Delta t\| < 5$ ns [%]	Mean Peak Efficiency [%]	Mean Time to Oscillations [ns]
Bare Aluminum	21	10 ± 5	51 ± 21
Velvet	37	15 ± 8	23 ± 7

shots having simultaneous peak output power from each SWS ($|\Delta t| < 5$ ns). The full operating range of the velvet emitter could not be explored because the electromagnets could not provide more than 0.32 T. Nonetheless, the ability of the magnetron with a velvet emitter to operate at considerably higher magnetic fields compared with that with the bare aluminum emitter is an interesting result. A possible explanation for this observation is the higher plasma closure velocity observed with velvet emitters [23]. Plasma expansion results in a smaller effective AK gap, which would require a higher B-field to achieve electron beam synchronism with the RF. Similar behavior has also been observed in [19]. In that study, the addition of end caps to the cathode led to both an increase in the peak magnetron power and an increase in the peak magnetic field at which the magnetron could operate.

The velvet emitter was also considerably more efficient, on average, than the bare aluminum emitter. As discussed previously, total instantaneous efficiencies were determined using the total current (including endloss). Specifically, the efficiency was determined by dividing the peak total output power by the product of current and voltage at the time of the peak total output power. Because of the slow MELBA-C voltage rise time, no inductive loss correction was needed. Table III shows that the velvet exhibited a 50% efficiency improvement over the aluminum emitter. High-power (>100 MW) shots exhibited peak instantaneous efficiencies between 12%–32%.

The last metric investigated was the oscillation start time. The reference time ($t = 0$) was the point on the rising edge at which the MELBA-C voltage pulse was half of the maximum. Table III shows the velvet decreased the mean time to the onset of oscillations by about 55%. This observation, combined with the general trend that the bare aluminum typically drew less current during the voltage ramp than the velvet up to the onset of oscillations, suggests the velvet emitter turned ON at lower electric fields than the bare metal. Apart from the increase in efficiency associated with operating at higher magnetic fields [19], another contributing factor to the velvet efficiency increase may stem from more uniform emission coupled with emission over a larger area, which reduces the localized current density. While the bare aluminum emitter surface area was larger, typically emission actually occurs from highly localized spots compared to velvet, which emits more consistently over its entire surface [24]. A reduction in current density has been shown to be associated with an increase in efficiency in simulations [25].

IV. CONCLUSION

As a first prototype of the RPM concept, the unoptimized unloaded experimental RPM-12A was initially prone to significant mode competition, which was exacerbated by the bifurcated mode structure intrinsic to an RPM [7]. In an attempt to promote frequency-locked operation between the two weakly coupled RPM-12A planar cavity arrays, the MCC was developed. Prior analytic and simulation work demonstrated that the MCC geometry, acting as both an emission-primed electron source and a resonant electromagnetic coupler, could promote frequency-locked operation and increase the frequency separation between the even and odd π modes [17].

This paper has experimentally demonstrated the efficacy of the MCC as a means of promoting frequency-locking relative to a solid planar cathode. In particular, for the frequency-locking criteria defined in Section III, the MCC-2 design improved the frequency-locking probability from 23% of shots to 57% of shots. While MCC-2 did show improvement, an ideal design would reduce both the AK gap and cathode thickness to increase the coupling between the planar oscillators.

To experimentally determine the power and efficiency of RPM-12A, a prototype coaxial microwave power extraction assembly was installed and tested using MCC-2 with either a bare aluminum or velvet dielectric electron emitter. The results showed that peak total output powers were similar for both emitters, but the velvet was considerably more consistent from shot to shot. In both cases, peak total output power was maximized only when both oscillators produced a maximum power within approximately 5 ns of each other, which occurred for 21% and 37% of shots for the aluminum and velvet emitters, respectively. The velvet emitter also reduced the mean time to oscillations from 51 ns (for the aluminum emitter) to 23 ns. The peak total efficiency for the velvet was, on average, 15%, a significant improvement over the aluminum efficiency of 10%. High-power (>100 MW) velvet shots exhibited between 12%–32% efficiency. While the endloss current was unknown for these shots, a similar configuration determined endloss was at most 200 A, which is low enough to suggest that the electronic efficiencies were not appreciably greater than the quoted total efficiencies.

During frequency-locked operation, each oscillator exhibited a frequency between 970 and 990 MHz. This represents the range of expected frequencies for the loaded even/odd π and even/odd $5\pi/6$ modes. However, implementation of the asymmetric power extraction scheme (with respect to the π and $5\pi/6$ modes), in conjunction with the MCC, created a complicated mode structure supported by the RPM that remained susceptible to mode competition during nonfrequency-locked shots. Mitigation of this competition is being explored in a future design featuring a symmetric all-cavity extraction technique [26], [27].

REFERENCES

[1] R. M. Gilgenbach *et al.*, “Heating at the electron cyclotron frequency in the ISX-*B* tokamak,” *Phys. Rev. Lett.*, vol. 44, no. 10, pp. 647–650, Mar. 1980. [Online]. Available: http://link.aps.org/doi/10.1103/PhysRevLett.44.647

[2] R. M. Gilgenbach, Y. Y. Lau, H. McDowell, K. L. Cartwright, and T. A. Spencer, “Crossed-field devices,” in *Modern Microwave and Millimeter-Wave Power Electronics*, R. J. Barker, J. H. Booske, N. C. Luhmann, Jr., and G. S. Nusinovich, Eds. Piscataway, NJ, USA: IEEE Press, 2005, ch. 6.

[3] G. B. Collins, Ed., *Microwave Magnetrons*. New York, NY, USA: McGraw-Hill, 1948.

[4] N. Friedman, *The Naval Institute Guide to World Naval Weapon Systems*, 5th ed. Annapolis, MD, USA: Naval Inst. Press, 2006.

[5] R. M. Gilgenbach, Y. Y. Lau, D. M. French, B. W. Hoff, J. Luginsland, and M. A. Franzi, "Crossed field device," U.S. Patent US 8 841 867 B2, Sep. 23, 2014.

[6] R. M. Gilgenbach, Y. Y. Lau, D. M. French, B. W. Hoff, M. A. Franzi, and J. Luginsland, "Recirculating planar magnetrons for high-power high-frequency radiation generation," *IEEE Trans. Plasma Sci.*, vol. 39, no. 4, pp. 980–987, Apr. 2011.

[7] M. A. Franzi *et al.*, "Recirculating-planar-magnetron simulations and experiment," *IEEE Trans. Plasma Sci.*, vol. 41, no. 4, pp. 639–645, Apr. 2013.

[8] B. W. Hoff, M. A. Franzi, D. M. French, G. B. Greening, and R. M. Gilgenbach, "A compact, pi-mode extraction scheme for the axial B-field recirculating planar magnetron," Air Force Res. Lab. Directed Energy Directorate, Albuquerque, NM, USA, Tech. Rep. AFRL-RD-PS-TR-2012-0039, Jul. 2012.

[9] M. R. López *et al.*, "Relativistic magnetron driven by a microsecond e-beam accelerator with a ceramic insulator," *IEEE Trans. Plasma Sci.*, vol. 32, no. 3, pp. 1171–1180, Jun. 2004.

[10] M. R. López, "Experiments on a relativistic magnetron driven by a microsecond electron beam accelerator with a ceramic insulating stack," Ph.D. dissertation, Dept. Nucl. Eng. Radiol. Sci., Univ. Michigan, Ann Arbor, MI, USA, 2003.

[11] B. W. Hoff, M. A. Franzi, R. M. Gilgenbach, and Y. Y. Lau, "Three-dimensional simulations of magnetic priming of a relativistic magnetron," *IEEE Trans. Plasma Sci.*, vol. 38, no. 6, pp. 1292–1301, Jun. 2010.

[12] B. W. Hoff, "Magnetic priming of a relativistic magnetron," Ph.D. dissertation, Dept. Nucl. Eng. Radiol. Sci., Univ. Michigan, Ann Arbor, MI, USA, 2009.

[13] M. A. Franzi, "Relativistic recirculating planar magnetrons," Ph.D. dissertation, Dept. Nucl. Eng. Radiol. Sci., Univ. Michigan, Ann Arbor, MI, USA, 2014.

[14] D. Price, J. S. Levine, and J. N. Benford, "Diode plasma effects on the microwave pulse length from relativistic magnetrons," *IEEE Trans. Plasma Sci.*, vol. 26, no. 3, pp. 348–353, Jun. 1998.

[15] M. C. Jones, V. B. Neculaes, Y. Y. Lau, R. M. Gilgenbach, and W. M. White, "Cathode priming of a relativistic magnetron," *Appl. Phys. Lett.*, vol. 85, no. 26, pp. 6332–6334, 2004. [Online]. Available: http://scitation.aip.org/content/aip/journal/apl/85/26/10.1063/1.1841454

[16] M. Fuks and E. Schamiloglu, "Rapid start of oscillations in a magnetron with a 'transparent' cathode," *Phys. Rev. Lett.*, vol. 95, no. 20, pp. 205101-1–205101-4, Nov. 2005. [Online]. Available: http://link.aps.org/doi/10.1103/PhysRevLett.95.205101

[17] M. A. Franzi, R. M. Gilgenbach, Y. Y. Lau, B. W. Hoff, G. B. Greening, and P. Zhang, "Passive mode control in the recirculating planar magnetron," *Phys. Plasmas*, vol. 20, no. 3, pp. 033108-1–033108-8, Mar. 2013. [Online]. Available: http://scitation.aip.org/content/aip/journal/pop/20/3/10.1063/1.4794967

[18] M. Unser, A. Aldroubi, and M. Eden, "Polynomial spline signal approximations: Filter design and asymptotic equivalence with Shannon's sampling theorem," *IEEE Trans. Inf. Theory*, vol. 38, no. 1, pp. 95–103, Jan. 1992.

[19] Y. M. Saveliev, S. N. Spark, B. A. Kerr, M. I. Harbour, S. C. Douglas, and W. Sibbett, "Effect of cathode end caps and a cathode emissive surface on relativistic magnetron operation," *IEEE Trans. Plasma Sci.*, vol. 28, no. 3, pp. 478–484, Jun. 2000.

[20] M. R. López *et al.*, "Cathode effects on a relativistic magnetron driven by a microsecond e-beam accelerator," *IEEE Trans. Plasma Sci.*, vol. 30, no. 3, pp. 947–955, Jun. 2002.

[21] T. A. Spencer, "High-current, long-pulse gyrotron-backward-wave oscillator experiments," Ph.D. dissertation, Dept. Nucl. Eng. Radiol. Sci., Univ. Michigan, Ann Arbor, MI, USA, 1991.

[22] T. A. Treado, R. S. Smith, III, C. S. Shaughnessy, and G. E. Thomas, "Temporal study of long-pulse relativistic magnetron operation," *IEEE Trans. Plasma Sci.*, vol. 18, no. 3, pp. 594–602, Jun. 1990.

[23] R. M. Gilgenbach *et al.*, "Microsecond electron beam diode closure experiments," in *Proc. IEEE Pulsed Power Conf.*, Jun. 1985, pp. 126–132.

[24] V. Vekselman *et al.*, "Plasma characterization in a diode with a carbon-fiber cathode," *Appl. Phys. Lett.*, vol. 93, no. 8, pp. 081503-1–081503-3, Aug. 2008. [Online]. Available: http://scitation.aip.org/content/aip/journal/apl/93/8/10.1063/1.2976136

[25] R. W. Lemke, T. C. Genoni, and T. A. Spencer, "Effects that limit efficiency in relativistic magnetrons," *IEEE Trans. Plasma Sci.*, vol. 28, no. 3, pp. 887–897, Jun. 2000.

[26] A. D. Greenwood, "All cavity magnetron axial extractor," U.S. Patent US 7 106 004 B1, Sep. 12, 2006.

[27] B. W. Hoff, A. D. Greenwood, P. J. Mardahl, and M. D. Haworth, "All cavity-magnetron axial extraction technique," *IEEE Trans. Plasma Sci.*, vol. 40, no. 11, pp. 3046–3051, Nov. 2012.

Matthew A. Franzi (S'09) received the B.S.E., M.S.E., and Ph.D. degrees in nuclear engineering with a minor in plasma physics from the University of Michigan (UM), Ann Arbor, MI, USA, in 2008, 2010, and 2014, respectively.

He was a Researcher with the Plasma, Pulsed Power, and Microwave Laboratory, UM, during his graduate studies, where he was focused on the development of relativistic magnetrons, in particular, the recirculating planar magnetron. He has been with the SLAC National Accelerator Laboratory, Menlo Park, CA, USA, since 2014, where he is currently involved in RF source development and the experimental testing of high gradient X-band accelerator structures.

Geoffrey B. Greening (S'12) received the B.S.E. and M.S.E. degrees in nuclear engineering and radiological sciences with a minor in plasma from the University of Michigan (UM), Ann Arbor, MI, USA, in 2010 and 2012, respectively, where he is currently pursuing the Ph.D. degree.

He has been with the Safeguards Laboratory, Oak Ridge National Laboratory, Oak Ridge, TN, USA, L-3 Communications Electron Devices, Williamsport, PA, USA, and the Directed Energy Directorate, Air Force Research Laboratory, Kirtland Air Force Base, Albuquerque, NM, USA. He is currently a Graduate Student Research Assistant with the Plasma, Pulsed Power, and Microwave Laboratory, UM, under the supervision of Prof. R. M. Gilgenbach. His research focuses on high-power microwave source development. His current research interests include multipactor discharges.

Nicholas M. Jordan (S'05–M'13) received the B.S.E., M.S.E., and Ph.D. degrees in nuclear engineering with a minor in plasma physics from the University of Michigan (UM), Ann Arbor, MI, USA, in 2002, 2004, and 2008, respectively.

He was with Cybernet Systems, Ann Arbor, where he was involved in microwave vehicle stopping technology, for five years, before returning to UM as an Assistant Research Scientist with the Plasma, Pulsed Power, and Microwave Laboratory in 2013. His current research interests include high-power microwave devices, pulsed power, laser ablation, Z-pinch physics, and plasma discharges.

Ronald M. Gilgenbach (LF'06) received the B.S. and M.S. degrees from the University of Wisconsin—Madison, Madison, WI, USA, in 1972 and 1973, respectively, and the Ph.D. degree in electrical engineering from Columbia University, New York, NY, USA, in 1978.

He spent several years as a member of the Technical Staff with Bell Labs, Murray Hill, NJ, USA, in the early 1970s. From 1978 to 1980, he performed gyrotron research with the Naval Research Laboratory, Washington, DC, USA, and also performed the first electron cyclotron heating experiments on tokamak plasma with the Oak Ridge National Laboratory, Oak Ridge, TN, USA. He joined as a Faculty Member with the University of Michigan (UM), Ann Arbor, MI, USA, in 1980, where he became the Director of the Plasma, Pulsed Power and Microwave Laboratory. He has supervised 46 graduate Ph.D. students with UM. He has collaborated in research with scientists at the Air Force Research Laboratory, Albuquerque, NM, USA, Sandia National Laboratories, Albuquerque, NASA Glenn, Cleveland, OH, USA, Northrop-Grumman, Falls Church, VA, USA, L-3 Communications, Williamsport, PA, USA, General Motors Research Labs, Ann Arbor, the Los Alamos National Laboratory, Los Alamos, NM, USA, Fermilab, Batavia, IL, USA, the Naval Research Laboratory, and the Institute of High Current Electronics, Tomsk, Russia. He is currently the Chair and Chihiro Kikuchi Collegiate Professor with the Department of Nuclear Engineering and Radiological Sciences, UM. He has authored over 165 articles in refereed journals and books, and holds five patents granted.

Dr. Gilgenbach is a fellow of the American Physical Society Division of Plasma Physics. He was a recipient of the NSF Presidential Young Investigator Award in 1984, and the Plasma Sciences and Applications Committee (PSAC) Award from the IEEE in 1997. He served as the PSAC Chair from 2007 to 2008. He was an Associate Editor of the *Physics of Plasmas* journal.

David H. Simon (S'10) was born in Sacramento, CA, USA. He received the B.S. degrees in mechanical engineering and nuclear engineering from the University of California at Berkeley, Berkeley, CA, USA, in 2007. He is currently pursuing the Ph.D. degree with the University of Michigan, Ann Arbor, MI, USA.

Y. Y. Lau (M'98–SM'06–F'08) was born in Hong Kong. He received the B.S, M.S., and Ph.D. degrees in electrical engineering from the Massachusetts Institute of Technology (MIT), Cambridge, MA, USA, in 1968, 1970, and 1973, respectively.

He was an Instructor and then an Assistant Professor of Applied Mathematics with MIT from 1973 to 1979. He was a Research Physicist with Science Applications Inc., McLean, VA, USA, from 1980 to 1983, and the Naval Research Laboratory, Washington, DC, USA, from 1983 to 1992. Since 1992, he has been a Professor with the Applied Physics Program and the Department of Nuclear Engineering and Radiological Sciences, University of Michigan, Ann Arbor, MI, USA. He has been involved in electron beams, coherent radiation sources, plasmas, and discharges. He has authored over 190 refereed publications. He holds ten patents. His current research interests include heating phenomenology, physics of quantum and higher dimensional diodes, Thomson X-ray sources, and electrical contacts.

Dr. Lau was elected as a fellow of the American Physical Society in 1986. He was a recipient of the Sigma-Xi Scientific Society Applied Science Award in 1989, and the IEEE Plasma Science and Applications Award in 1999. He served three terms as an Associate Editor of the *Physics of Plasmas* journal. He was a Guest Editor of the IEEE TRANSACTIONS ON PLASMA SCIENCE of the Special Issue on High Power Microwave Generation.

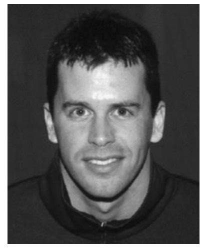

Brad W. Hoff (S'04–M'10) received the B.S. degree in physics from the U.S. Naval Academy, Annapolis, MD, USA, in 1999, and the M.S.E. degrees in nuclear engineering and electrical engineering, and the Ph.D. degree in nuclear engineering from the University of Michigan, Ann Arbor, MI, USA, in 2006, 2007, and 2009, respectively.

He is currently a Research Physicist with the Directed Energy Directorate, Air Force Research Laboratory, Kirtland Air Force Base, Albuquerque, NM, USA. His current research interests include high-power microwave sources and directed energy technology.

John Luginsland (S'95–M'96) received the B.S.E., M.S.E., and Ph.D. degrees in nuclear engineering with a minor in plasma physics from the University of Michigan, Ann Arbor, MI, USA, in 1992, 1994, and 1996, respectively.

He was a National Research Council Resident Research Associate with the Advanced Weapons and Survivability Directorate, Air Force Phillips Laboratory, Albuquerque, NM, USA, in 1996, and a Staff Member with the Plasma Physics Branch, Directed Energy Directorate, Air Force Research Laboratory, Albuquerque, until 2001. From 2001 to 2003, he was with Science Applications International Corporation, McLean, VA, USA, where he was involved in advanced pulsed-power applications. From 2003 to 2009, he was with NumerEx, Limited Liability Company, Albuquerque. Since 2009, he has been with the Air Force Office of Scientific Research, Arlington, VA, USA, where he is currently the Program Manager for fundamental research on plasma and electro energetic physics with a focus on directed energy, nonequilibrium plasma, and high-energy density pulsed-power physics. His current research interests include theoretical and computational plasma physics from the kinetic to magnetohydrodynamic limits, electromagnetism, and fluid dynamics with applications to advanced survivability concepts, accelerator schemes, combustion research, and various types of radiation production.

Dr. Luginsland was a recipient of the IEEE Nuclear and Plasma Sciences Society (NPSS) Early Achievement Award in 2006. He was the Chair of the IEEE NPSS Plasma Science and Applications Committee.